Available online at www.sciencedirect.com

ScienceDirect

Procedia CIRP 62 (2017) 287 – 292

www.elsevier.com/locate/procedia

10th CIRP Conference on Intelligent Computation in Manufacturing Engineering - CIRP ICME '16

Single grain grinding: an experimental and FEM assessment

Guerrini G.[a], Bruzzone A.A.G*[b], Crenna F[b]

[a]School of Industrial Engineering, University of Bologna, Bologna, Italy

[b]Department of Mechanical Engineering, Energetics, Management and Transportation, Polytechnic School, University of Genoa, Genoa, Italy

* Corresponding author. Tel.: +39-0103532894; fax: +039-010-317750. *E-mail address:* Alessandro.Bruzzone@unige.it

Abstract

Peripheral grinding is inherently complex due to peculiar factors such as: the non deterministic microgeometry of the grinding wheel, the composition of the grinding wheel, essentially non homogeneous, the cutting process dynamics, where the grains' cutting edges operate on a surface whose microgeometry is the result of the cutting actions of the preceding abrasive grains.
This paper compares the results of the experimental analysis of the effect of single cutting grains on the actual microgeometry of worked surfaces, and the results obtained by a FEM cutting model where the measured microgeometry of the cutting grains is considered.

Peer-review under responsibility of the scientific committee of the 10th CIRP Conference on Intelligent Computation in Manufacturing Engineering

Keywords: surface; grinding; model

1. Introduction

Complexity of grinding process represents a demanding challenge to researchers looking to establish a relationship between the process parameters, the surface quality, the process dynamic and the tool wear.

The complexity is basically due to the stochastic features characterizing the grinding wheel: the grain shape, their geometrical distribution within the bounding cement, the chemo-physical characteristics of the grinding wheel materials. Furthermore the high cutting speed and the micrometric scale of the interaction between the workpiece material and the active section of the grinding wheel make the experimental observation of the phenomenon really difficult.

Several grinding models have been proposed in literature: physical process models (analytical and numerical models), empirical process models (regression analysis, artificial neutral net models) as well as heuristic process models (rule based models) [1, 2, 3].

In order to face the complexity of the grinding process this paper presents a preliminary study based on the experimental observation of the single grain grinding; the obtained results provide a guide for the validation of a 3D FEM model. The grains geometry, acquired by using a stylus instrument, is employed by the FEM model to analyse the interaction between the cutting grain and the workpiece.

The proposed methodology, although possibly being objected due to the actual limit of the real grain geometry measuring system, is a suitable approach to model the interaction between a single grain and the grinded surface.

2. Methodology and experimental set-up

2.1. Methodology

This study follows the approach shown in Figure 1. Specifically the methodology is based on the development of a dynamometer able to be used instead of the grinding wheel: the dynamometer carries the grain on a changeable fixture. Once the grain's geometry is acquired, the grinding cutting forces are measured. 3D FEM runs considering the grain's acquired geometry as well as the actual process parameters in order to compute cutting forces and temperature. Also the surface profile obtained by the single grain grinding is acquired and the measured depth is used to estimate the maximum depth of the chip and the specific cutting force.

Peer-review under responsibility of the scientific committee of the 10th CIRP Conference on Intelligent Computation in Manufacturing Engineering
doi:10.1016/j.procir.2016.07.082

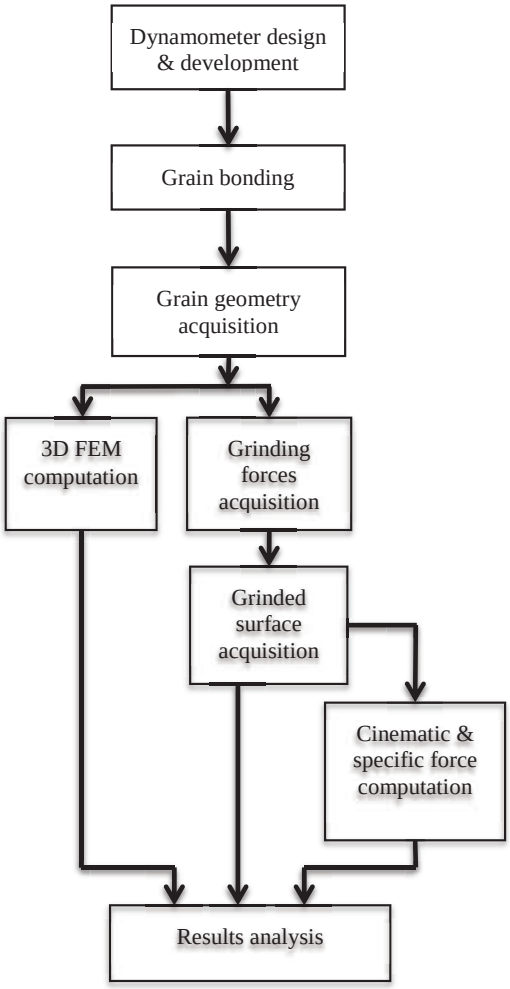

Fig. 1. Structure of the single grain grinding study.

2.2. Dynamometer design & development

Compressive (F_z) and tangential (F_x)forces acting on the single grain were acquired by using a dynamometer whose geometry is shown in Figure 2. Basically the spring consists of a tubular shaft connected through a bushing to the spindle. On the opposite shaft end there is a threaded hole holding a M4 screw that provides the surface where one or more abrasive grains can be glued.

Two full strain gage bridges are bonded on the tubular shaft; power supply and bridges' signals are connected to the AD system by using a slip ring (Michigan Scientific).

The dynamometer is characterized by symmetric geometry to avoid balancing issues: a dummy tubular rod permits to reduce vibrations during the spindle rotation.

2.3. Abrasive grains and bonding

Fused aluminium oxide (Al_2O_3) conventional abrasive was used. This abrasive is designed for grinding long chipping, ductile materials such as steels and super alloys. The fused aluminium oxide grains have a Knoop-Hardness of 19 GPa, and are characterized by an undefined geometry. These grains are designed to crack down when the forces exceed a certain value in order to create new cutting edges reducing the effect of wear; the grains usually break down after four cutting cycles providing new sharp cutting edges.

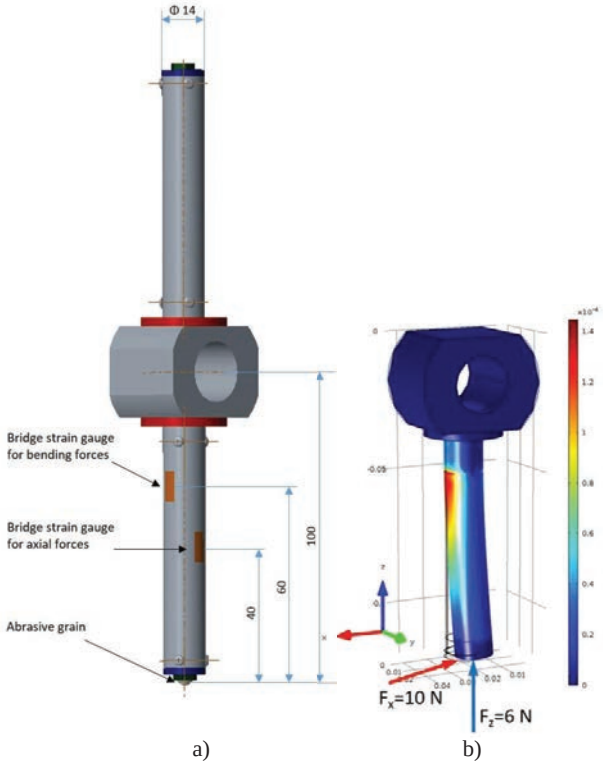

Fig. 2. Dynamometer: a) geometry, b) deformation due to tangential force.

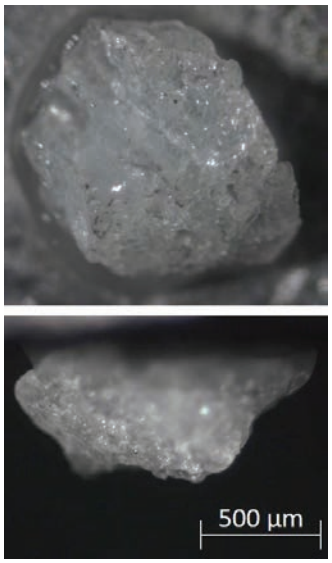

Fig. 3. Grain glued on the screw: bottom and front view.

A grit size of 16 was used since bigger grain size simplifies the gluing procedure used to mount the grain on the dynamometric tool developed for the tests (Figure 3).

Each grain has been glued on the head of a screw that could be fastened to the threaded hole of the measuring tool. Epoxy adhesive was used to glue the grit on the screw head providing a stiff bond to avoid the grain separation during grinding tests; actually 15 grit-screw couples have been used in the test.

2.4. Grain geometry acquisition

Microgeometry of the bonded grains have been acquired by using a 3D contact stylus (Taylor Hobson Talyscan 150); the stylus cone has a tip angle $\theta = 90°$ and tip radius $r = 2$ μm; sampling length was $\Delta x = \Delta y = 5$ μm.

The stylus geometry acts as a mechanical low pass filter that impedes a correct acquisition of the actual geometry. Essentially surfaces with slope greater than $\theta/2 = 45°$ cannot be measure as well as the undercuts that characterize grinding wheels surface microgeometry. Unfortunately this issue cannot be faced with the metrological systems usually employed in manufacturing research. In order to estimate the actual slope of the grain geometry each bonded grain was observed and measured through optical microscope observing a mean slope value of 27.5±29°.

2.5. Workpiece material

An alloyed case hardening steel (20MnCr5) was chosen as workpiece material for its industrial relevance. This material is typically used for parts requiring core tensile strength of 1000-1300 MPa and good wearing resistance such as spindles, camshafts, gears and shafts; these parts always require very good surface finishing obtained by grinding. The workpiece material was cut in samples and each of them was polished in order to obtain a mirror finished plane surface. On each sample more than one grinding pass was performed. A custom holding plate was also designed to ensure the right positioning of the sample on the worktable of the grinding machine.

2.6. AD acquisition system and parameters

The tangential and compressive forces were measured through two full strain gauge bridges conditioned by a National Instruments SCXI 1121 power supply amplifier, with gain 1000, and a PXI-MIO 16E1 12 bit data acquisition board. A LabView ® program was developed to acquire and save the data with a sampling frequency of 100kHz.

The complete measurement chains, including acquisition software, were statically calibrated applying a set of reference masses to the dynamometer in the same point were the grain is positioned during normal measurements. Calibration was repeated during the measurement campaign to verify sensors stability. Each acquisition corresponds to 7 s time history of compressive and tangential forces. Acquired signals were therefore processed in order to discard the initial part where the grain begins to cut the material and the final portion where the grain leaves the sample surface.

Fig. 4. Experimental set-up for the grinding tests.

2.7. Cutting parameters

The grinding parameters used for the tests were: spindle revolutions S = 2800 rpm, cutting speed $v_c = 29.3$ m/s, feed rate f = 8.6 mm/s, depth of cut a_e = 20-50-100 μm.

All the tests were performed with a discordance set up for several cutting cycles in order to grind the entire length of the workpiece without changing the cutting depth.

For each of the 15 cutting grains two tests were repeated at each cutting depth. Figure 4 shows the set-up used for the grinding tests.

3. FEM model

A finite element model (FEM) of the interaction between a single abrasive grain and steel workpiece has been developed using the software package DEFORM 3D. The acquired geometries of the abrasive grains used in the experiments were reproduced as 3D volume CAD models and introduced into the FEM software to calculate cutting forces; Figure 5 shows the cutting grain geometry acquired by using the 3D stylus instrument for the grain represented in Figure 3.

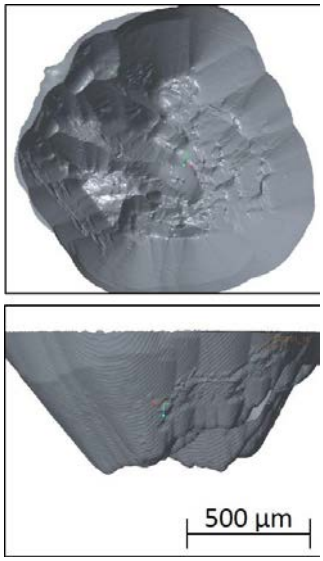

Fig. 5. Top a) and lateral b) views of the cutting grain geometry acquired for the grain of Fig. 3.

Tab. 1. Main FEM simulation parameters.

	Material	Geometry	Movements	Mesh
Work-piece	20MnCr5 (plastic)	Rectangular 10x3x2 mm	Fixed X Y Z	Min 1/3 a_e
Grinding Tool	Al_2O_3 (rigid)	Real grain geometry	Ω_c=2800rpm v_c= 29.3 m/s f = 8.6 mm/s	Min 1/3 a_e
Johnson and Cook constants according to "20MnCr5"				

Due to the low depth of cut compared to machining performed with defined-geometry tools such as turning, as well as the high translational velocity of the abrasive grain, a set of preliminary simulations was first performed in order to optimize the mesh geometry and time step.

In order to improve computational efficiency, separate mesh windows were created, corresponding to the tool, zone of interaction and bulk material, respectively, with tetrahedral elements optimized in size within the zone of interaction so as to accurately reproduce the cutting forces and chip development.

Automatic remeshing was performed according to a maximum element penetration depth between the work piece and abrasive grain. In order to further simplify the simulation, particularly in the case of multiple cutting passes, both rotation and translational velocity components were imposed on the abrasive grain while the work piece was held stationary by applying fixed boundary conditions along its base. Model outputs included the vertical and tangential cutting force components, as well as the temperature distribution in both the abrasive grain and the work piece.

The constitutive law used to model the plastic behavior of the workpiece material under the load of the grinding grain is the Johnson and Cook model of the flow stress σ_y:

$$\sigma_y\left(\varepsilon_p, \dot{\varepsilon_p}, T\right) = \left[A + B\left(\varepsilon_p\right)^n\right]\left[1 + C\ln\left(\dot{\varepsilon_p}^*\right)\right]\left[1 - (T^*)^m\right]$$

where $\varepsilon_p$is the equivalent plastic strain, $\dot{\varepsilon_p}$ is the plastic strain-rate, *A*, *B*, *C*, *n*, *m* are material constant and $\dot{\varepsilon_p}^*$ and T* are respectively the normalized strain-rate and temperature. The simulation parameters are listed in Table 1.

4. Results and discussion

4.1. Grain geometry

Considering grain geometry the most important parameter that should be examined is the rake angle; actually the undefined shape of the grain as well as its orientation provide a large dispersion of values. Figure 6 shows the microscope images of the top and lateral view of three cutting grains and the corresponding geometries acquired by using the stylus instrument. It could be observed that the rake angles resulting from the acquired grains geometry differ from the actual geometry due to the stylus tip angle. The acquired geometries have a maximum rake angle of -45° while the actual rake angles varies between -72° and +21°.

4.2. Measured forces

By using the instrumented tool cutting forces have been acquired. Maximum compressive (F_z) and tangential (F_x) forces measured for depths of cut a_e = 20-50-100 μm are reported in Table 2. Values refer to the first peak within each cutting passage; the contact time Δt between the workpiece and the grain for a_e = 50 μm is theoretically Δt = 2.16e-04 s. Measurement uncertainty is given with 68.27% probability.

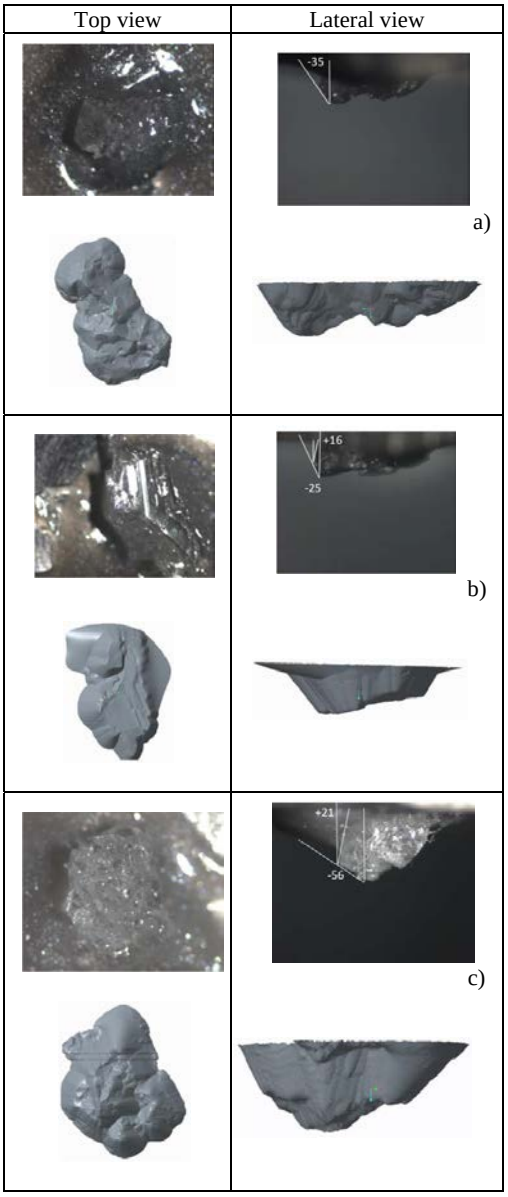

Fig. 6 Cutting grains: top, lateral views and corresponding stylus models.

Tab. 2 Measured compressive F_z and tangential F_x forces (mean values) for maximum depth of cut a_e.

Depth of cut a_e	Force [N]	
[μm]	F_z Compressive	F_x Tangential
20	43.3±20.9	2.8±1.2
50	76.3±46.4	4.4±2.6
100	122.9±71.7	6.9±2.9

Tab. 3. Computed maximum compressive Fz and tangential Fx forces (mean values) for maximum depth of cut a_e.

Depth of cut a_e	Force [N]	
[μm]	F_z Compressive	F_x Tangential
20	46.75±9.12	28.88±5.65
50	76.78±7.23	50.23±4.51
100	149.8±28.9	113.58±7.15

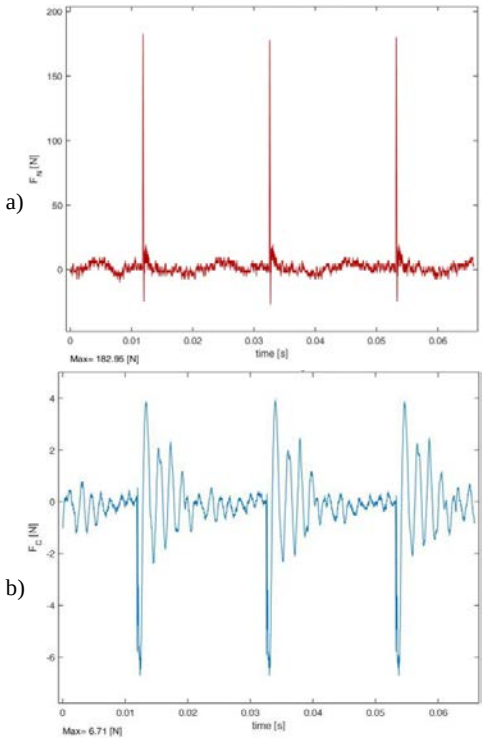

Fig. 7. Compressive F_z a) and tangential F_x b) force vs. time.

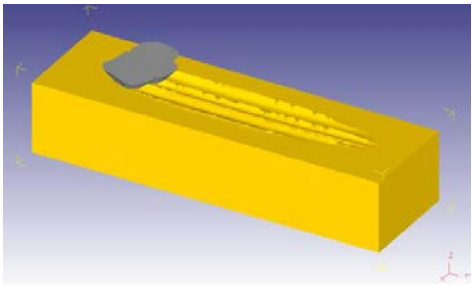

Fig. 8. Workpiece-grain interaction, a_e = 100 μm, first grain pass.

Figure 7 shows the compressive F_z a) and tangential F_x b) forces as a function of time for a depth of cut a_e = 50 μm. The damping behavior in the tangential component seems due to the mechanical characteristics of the dynamometric system.

4.3. FEM computed forces

Maximum compressive and tangential forces computed by using the 3D FEM model are reported in Table 3. Values relate to the fifth grain's pass. Simulation for each grain geometry takes about nine days on a I7 3.3 GHz workstation.

Figure 8 shows the corresponding workpiece-grain interaction provided by the model. Figure 9 displays the colormap of the equivalent Von Mises stress on the sample surface on a) the x-y plane, b) the x-z section and c) the temperature distribution.

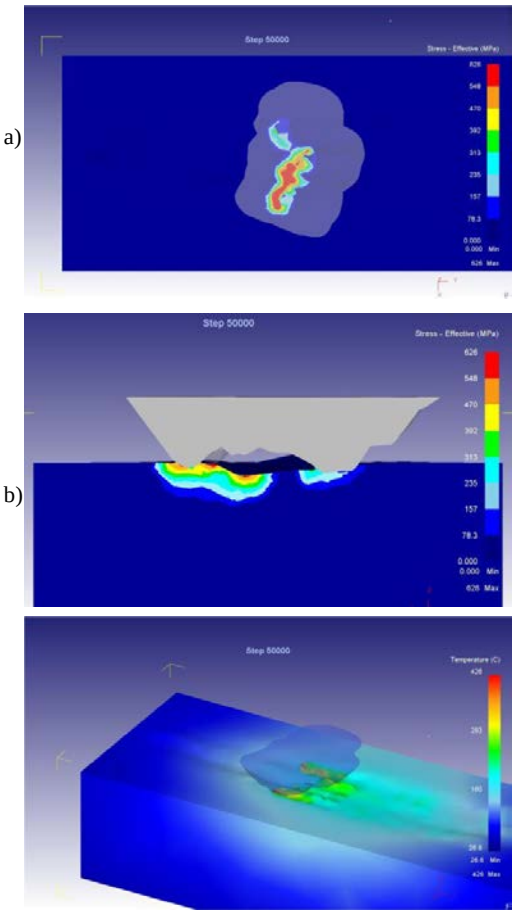

Fig. 9. Colormaps for ae = 100 μm grinding simulation of: a) the equivalent stress in the xy plane ; b) in the xz section of the workpiece; c) temperature distribution.

4.4. Surface profile

Profiles of surfaces obtained by the cutting tests have been acquired by using a Talyscan 150 stylus instrument. Figure 10 shows the actual a) and FEM b) profiles for a_e = 50 μm.

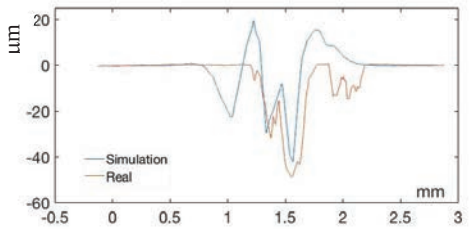

Fig. 10. Surface profile for a_e=50 µm: a) acquired with stylus instrument; b) computed by simulation.

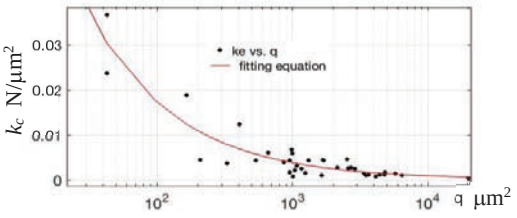

Fig. 11. Specific tangential cutting force kc vs chip sectional area q.

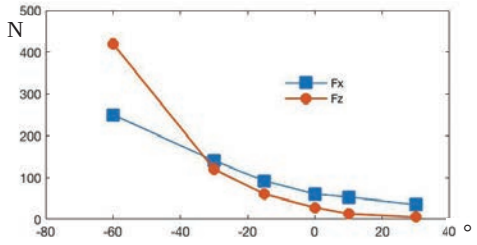

Fig. 12. Tangential F_x and compressive F_z components of cutting force.

4.5. Cinematic & dynamic forces

Considering a cinematic model, the maximum chip thickness h_{max} is given by the relationship:

$$h_{max} = 2 \cdot f_z \sqrt{a_e / D}$$

where a_e is the depth of cut, f_z = 180 µm/edge is the feed per grain and D = 200 mm is the diameter of the cutting edge path. The groove profile permits to estimate the real a_e, the maximum chip thickness and the maximum chip sectional area q corresponding to the actual cutting grain. Accordingly the maximum chip sectional area q for different depth of cut can be computed. Experimental data indicate that q is in the range 40-20000 µm^2 for the real a_e. Figure 11 shows the specific tangential force ($k_c = F_x/q$) and the fitting equation:

$$k_c = 0.34 \cdot q^{-0.65}$$

with q measured in µm^2 and k_c in N/µm^2. The experimental values are in accordance with those reported in literature [4].

4.6. Discussion

Meanwhile compressive forces acting on the cutting grain have experimental values comparable to those provided by the FEM simulation, the measured tangential forces are quite below those provided by the simulation. This difference is possibly due to three factors:

- the difference between the actual grain geometry an the acquired geometry used by the FEM model;
- the actual materials properties, such as friction between grain and workpiece, that could differ from those used by the FEM model;
- the metrological characteristics of the dynamometer that could perform as a mechanical low pass filter for the force component along the tangential direction.

Indeed the actual rake angle plays a fundamental role in the cutting dynamics. Figure 12 shows the effect of the rake angle on the tangential and compressive components of the cutting force resulting from a 2D FEM simulation carried out considering the same workpiece material and cutting parameters. Since according to the simulation the rake angle influences both the tangential, both the compressive force, the causes of the measured lower tangential force values could not be confidently only attributed to the differences between the real and the measured rake angle.

In order to assess the dynamometer's influence on the tangential force values, a reference dynamometric cell directly holding the workpiece should be used to measure the force components.

Friction coefficient is another factor that possibly explains the differences; furthermore the scale effect on the material behavior during the cutting process could play an important role: according to Figure 11 as the chip sectional area decreases, the specific tangential force increases.

5. Conclusion

This ongoing study foresees the comparison of simulated and experimental cutting forces in order to more accurately predict the principal factors influencing the grinding process.

The differences observed in this study point out two main open issues that should be addressed in future experimental work: the necessity of a sound acquisition of the real grain geometry and an accurate characterization of the mechanical properties of the materials and their interaction at the dimensional scale characterizing the grinding process.

References

[1] Brincksmeier E et al. Advances in Modeling and Simulation of Grinding Processes. CIRP Annals – Manufacturing Technology 2006; 55: 667-30.
[2] Tonshoff HK, Friemuth T, Becker JC. Process monitoring in grinding. CIRP Annals 2002; 51: 551-21.
[3] Opoz TT, Chen X. Experimental investigation of material removal mechanism in single grit grinding. Int J of Machine Tools and Manufacture 2012; 63, December: 32-9.
[4] Transchel R. Cutting mechanism of active brazed single diamond grains. Dr. thesis Diss. ETH no. 22156 2